

Wearable Pulse Oximetry in Construction Environments

by

Jason B. Forsyth

Thesis submitted to the Faculty of the
Virginia Polytechnic Institute and State University
in partial fulfillment of the requirements for the degree of

Master of Science
in
Computer Engineering

Thomas L. Martin, Chair
Deborah E. Young-Corbett
Edward A. Dorsa

March 29, 2010
Blacksburg, Virginia

Keywords: Pulse Oximetry, Wearable Computing, Carbon Monoxide

Copyright 2010, Jason B. Forsyth

Wearable Pulse Oximetry in Construction Environments

Jason B. Forsyth

(ABSTRACT)

The goal of this project was to determine the feasibility of non-invasively monitoring the blood gases of construction workers for carbon monoxide exposure. A blood gas sensor was integrated into a typical construction helmet to determine the feasibility of monitoring workers for carbon monoxide exposure throughout the day. In particular, this study sought to understand the impact of motion artifacts caused by the worker's activities and to determine if those activities would prevent the blood gas sensor from detecting the onset of carbon monoxide poisoning. This feasibility study was conducted using a blood oxygen sensor rather than a blood carbon monoxide sensor for several reasons. First, blood gas sensors that measure blood carbon monoxide are not readily available in suitable physical form factors. Second, sensors for blood oxygen and blood carbon monoxide operate on the same physical principles and thus will be affected in the same way by worker motions. Finally, using a blood oxygen sensor allowed the study to be conducted without exposing the human subjects to carbon monoxide. A user study was conducted to determine the distribution of motion artifacts that would be created during a typical work day. By comparing that distribution to a worst-case estimate of time to impairment, the probability that helmet will adequately monitor the worker can be established. The results of the study show that the helmet will provide a measurement capable of warning the user of on setting carbon monoxide poisoning with a probability greater than 99%.

Acknowledgments

I am indebted to many people for the completion of this work:

To the ECE 5564: Wearable and Ubiquitous Computing class during the Fall 2008. Along with my group members, Khanh Duong, Ramya Narayanaswamy, and Sureshwar Rajagopalan, the major background work researching pulse oximetry and determining the feasibility of this project was developed in that class.

To the participants of the user study who endured wearing an odd helmet around campus. Without them, there would be no results, and hence no Master's thesis.

To Katie, my intrepid reviewer and best friend.

To my committee members Dr. Young-Corbett and Professor Dorsa for their guidance and direction throughout this project.

Finally, to my Advisor Dr. Martin for his constant support and encouragement which truly made this work possible.

This material is based in part upon work supported by the National Science Foundation under Grant Number EEP-0935103. Any opinions, findings, and conclusions or recommendations expressed in this material are those of the author(s) and do not necessarily reflect the views of the National Science Foundation.

Additionally, funding was received from the Center for Innovation in Construction Safety and Health Research at Virginia Tech for the purchase of a Masimo CO-pulse oximeter.

Contents

1	Introduction	1
1.1	Motivation	1
1.2	Methodology	2
1.3	Contributions	3
1.4	Thesis Organization	4
2	Background	5
2.1	Carbon Monoxide Poisoning	5
2.1.1	Physiological Effects	5
2.1.2	Workplace Incidents and Prevalence	6
2.2	Physiology of Pulse Oximetry	7
2.2.1	Measurement of COHb	8
2.3	Issues in Pulse Oximeter Design	9
2.3.1	Transmission and Reflective Oximeters	9
2.3.2	Motion Artifacts	11
2.4	Review of Helmet-Based Oximetry	12
3	Methodology & Uptake Estimation	13
3.1	Determining Prototype Reliability	13
3.2	Probabilistic Model of Sensor Performance	15

3.2.1	Gap Conditions	16
3.3	Prediction of Carbon Monoxide Uptake	17
3.3.1	The CFK Equation	17
3.3.2	CFK Parameters and Units	18
3.3.3	Solutions to CFK	19
3.4	Determination of Worker Profile	20
3.5	Time to Impairment and Incapacitation	22
4	Prototype Development & User Study	24
4.1	Physiological & Wearability Requirements	24
4.1.1	Wrist & Finger	25
4.1.2	Facial Regions	26
4.1.3	Selection of Forehead	26
4.2	Substitution of SpCO for SpO ₂	27
4.3	Helmet Prototype	28
4.4	Headband Design	28
4.4.1	Motion Issues	29
4.5	Electronics & Placement	31
4.5.1	Communication & Power	31
4.5.2	Energy Consumption	33
4.5.3	Placement Considerations	35
4.6	User Study	35
4.6.1	Selection of Tasks	36
4.6.2	Selection of Participants	36
4.6.3	Walking and Stairs	36
4.6.4	Sweeping	37
4.6.5	Hammering and Boxes	37

5 Results	38
5.1 Validating Helmet Reliability	38
5.1.1 Choice of Distribution	42
5.2 Helmet Performance Factors	42
5.2.1 Activities and Total Gap Size	45
5.2.2 Users and Total Gap Size	46
5.3 User Parameters	47
6 Conclusion	49
6.1 Future Work	50
Bibliography	51

List of Figures

2.1	PPG Signal from Pulse Oximeter	7
3.1	Measurement Gaps Induced by Hammering	14
3.2	Carbon Monoxide Uptake at 1200ppm	23
4.1	Interior and Back of Helmet Prototype	29
4.2	Modified Helmet Headband	30
4.3	Motion Induced Errors in PPG	30
4.4	Schematic of Prototype Components	32
4.5	High Gain Xbee Antenna	33
4.6	User Study Activities	37
5.1	Distribution of Gaps from User Study	39
5.2	Histogram Fitted with Lognormal Distribution	40
5.3	Various Distributions Mapped to Histogram	43
5.4	Individual Activity Contribution to Total Gap Time	46
5.5	Total Gap Size as Percentage of Activity Duration	47

List of Tables

3.1	Parameters of the CFK Equation	18
3.2	Profile of Typical and At-Risk Workers	21
3.3	Respiratory Exercise Parameters for Various Intensities	21
3.4	Time to Impairment (30% COHb) and Incapacitation (60% COHb) in Minutes at 1200 ppm	22
4.1	Comparison of Various Sensor Placements	25
4.2	System Lifetimes in Hours of Current and Future Deployed De- signs for Linear and Switching Regulators	34
5.1	Metrics of Fit to Histogram	42
5.2	User Performance: Average, Maximum, Total Gap in Seconds . .	43
5.3	User Performance: Average, Maximum, Total Gap in Seconds . .	44
5.4	Activity Durations in Minutes for Each User	44
5.5	Total Gap Organization for Friedman Analysis	45
5.6	Results of Friedman's Test	45
5.7	Grouping of Users by Total Gap Size	46

Chapter 1

Introduction

1.1 Motivation

Carbon monoxide poisoning is a significant problem for construction workers both in residential and industrial settings. Reviewing carbon monoxide poisonings in Washington State, Lofgren [1] found the construction industry second to only wholesale workers in the number of reported incidents. Furthermore, of the construction related inhalation deaths from 1990 to 1999, nearly 20% were due to carbon monoxide poisoning [2].

This danger exists because the exhaust from gasoline-powered hand tools can quickly build up in enclosed spaces and easily overcome not only the tool's user but co-workers as well. The construction population is at significant risk because initial symptoms of carbon monoxide poisoning such as headache, fatigue, and muscle ache, can easily be dismissed as part of the work day and not as indicators of something worse.

While this danger is known, current safety systems only monitor environmental concentrations of carbon monoxide. This is a huge liability as carbon

monoxide exposure affects people at different rates based on their activity level, body size, and most significantly their background risk factors such as smoking or anemia [3]. Thus environmental monitoring alone will not save the worker who is a daily smoker, or the person who has been sick and has a reduced red blood count as they may be overcome by carbon monoxide well before the environmental concentrations rise to the level of concern for their co-workers. In a large population like construction workers, it is impossible to estimate all the potential physiological factors that will affect each individual worker, therefore a method must be created that monitors all workers individually to avoid the shortcomings of environmental monitoring.

To correct this problem, a non-invasive blood oxygen sensor, called a pulse oximeter, has been integrated into a typical construction helmet to allow real-time monitoring of workers. Taking readings off the forehead of the wearer, the sensor is integrated into the headband of the helmet in such a way that the worker will only know it is present when alerted to danger and will otherwise go unnoticed. As will be further explained in Chapter 4, this study was conducted with a blood oxygen sensor rather than a blood carbon monoxide sensor for several reasons. First, blood gas sensors that measure blood carbon monoxide are not readily available in suitable physical form factors. Second, sensors for blood oxygen and blood carbon monoxide operate on the same physical principles and thus will be affected in the same way by worker motions. Finally, using a blood oxygen sensor allowed the study to be conducted without exposing the human subjects to carbon monoxide.

1.2 Methodology

To provide reliable coverage of the population the helmet prototype must be able to accurately measure the worker's internal carbon monoxide levels and warn

the user before becoming impaired from exposure. However, since the worker and helmet are constantly undergoing motion, the sensor may have difficulty in obtaining a measurement because of the amplitude and duration of motion, resulting in “gaps” in the sequence of measurements. As the worker will not be overcome immediately from carbon monoxide exposure, reliable coverage can also be expressed as showing that no measurement gap is longer than the worst-case time to impairment for a worker. This condition implies the existence of a valid measurement before the worker becomes impaired, which then can be used to warn the user or alert co-workers.

While the reliable coverage condition cannot be proven directly, the behavior of measurement gaps can be estimated by performing a user study involving typical construction tasks and analyzing the data to determine how often and of what duration gaps can occur. Combining this information with a hard limit for time to impairment (T_i), the series of gaps can be mapped to a probability distribution to directly answer how likely an event longer than T_i may occur. Thus the answer to how well the helmet protects combines an estimate of T_i as well as a probabilistic estimate of the gap distribution. This methodology will be expanded further in Chapter 3.

1.3 Contributions

This work presents a novel analysis of the reliability of helmet-based pulse oximetry while undergoing motion. While previous works have explored the use of pulse oximetry during motion [4] [5], no study has classified the behavior of motion artifacts to determine the reliability of obtaining a valid measurement. Here we describe the performance of the oximeter as a repairable system with a lognormal distribution of repair times. Using this distribution, we can compare the distribution of artifacts to determine the probability of receiving a

measurement before a worker becomes impaired.

1.4 Thesis Organization

The following chapters will outline the particular steps required to determine the feasibility of the helmet prototype. Chapter 2 provides further background on carbon monoxide exposure and overviews the basis of pulse oximetry. Chapter 3 presents the methodology and analytical tools used to determine the reliability of the prototype, along with estimations of impairment times for various workers. Chapter 4 describes the construction of the helmet prototype, and the user study conducted to validate the helmet. Chapter 5 presents the results of the user study. Finally, Chapter 6 concludes the work.

Chapter 2

Background

Designing a wearable medical device for the construction population involves a highly interdisciplinary approach involving human physiology, carbon monoxide uptake simulation, wearable computing, and reliability analysis. Providing the history and background for each subject is unnecessary as each subject is much larger than the methods required in this project. To that end, not all subjects will be reviewed, but supporting related work will be provided. This chapter will focus reviewing the motivation for monitoring construction workers as well as providing an overview of the key technology used, pulse oximetry. Finally, a comparison between our helmet based monitoring system and others is provided.

2.1 Carbon Monoxide Poisoning

2.1.1 Physiological Effects

Carbon monoxide is a colorless, odorless gas that is highly toxic to both humans and animals. When inhaled, carbon monoxide competes directly with oxygen in binding with hemoglobin. Carbon monoxide has an affinity for hemoglobin

over 200 times greater than oxygen [6, p.43]. This binding creates a new dysfunctional hemoglobin called carboxyhemoglobin (COHb) and greatly reduces the number of potential oxygen carrying hemoglobins (HbO₂). If the concentration of carboxyhemoglobin becomes too great, normal oxygen transport is interrupted, leading to cellular hypoxia and eventually death.

While the effects of carbon monoxide vary with internal concentrations, at 30% saturation the low level effects include headache, fatigue, and fainting. At higher levels, approaching 60%, a person will become unconscious and if not rescued, continued exposure will result in death [3].

As carbon monoxide diffuses in both directions across the lung-blood barrier, if presented with oxygen, a person will eventually exhale the carbon monoxide present in their body and recover [3, p.1466].

2.1.2 Workplace Incidents and Prevalence

Carbon monoxide exposure is a grave concern in the construction environment because it is readily present and the symptoms of its onset can easily be ignored. Created by incomplete combustion, carbon monoxide is produced by any gasoline powered tool such as saws, power washers, drills, and generators that are common on construction sites.

A report by NIOSH [7] highlights the danger of carbon monoxide exposure to construction workers. The majority of cases described involve workers using individual power hand tools such as pressure washers, or concrete saws. In a majority of cases workers were overcome in less than 30 minutes. Additionally, some workers knew of the danger and attempted to ventilate the areas, however their efforts were not sufficient.

2.2 Physiology of Pulse Oximetry

To monitor workers for the presence of carbon monoxide, pulse oximetry is used to non-invasively measure hemoglobin concentrations within the body. Pulse oximetry is an approximation of Beer's Law which relates the attenuation of light through a medium based upon the compounds it passes through. In the case of pulse oximetry, as light is shone through vascular tissue, it is absorbed at different rates and frequencies for each species of hemoglobin. Typically a pair of light emitting diodes (LED) and a photo detector (PD) are used to construct the oximeter.

In using pulse oximetry, a photopleysmograph (PPG) is created, showing the volumetric changes of blood through the monitoring site. The PPG rises and falls as the heart pumps blood through the body. A typical PPG signal is shown in Figure 2.1.

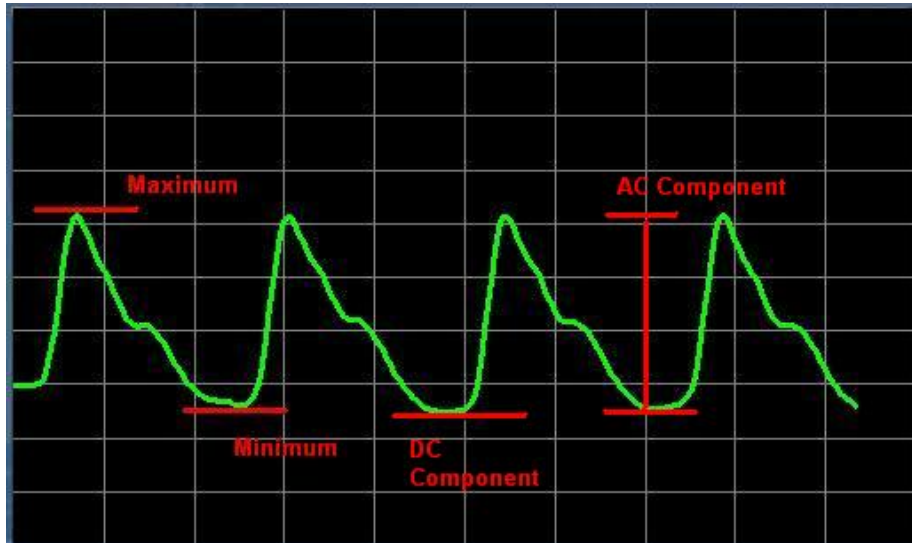


Figure 2.1: PPG Signal from Pulse Oximeter

The ingenuity of pulse oximetry is that it uses the maximum and minimum values of the PPG or “AC component” of the signal to determine attenua-

tion caused by pulsating blood only. This removes the “DC offset” of constant absorbers in the body such as venous blood, tissue, and pigmentation. Furthermore, using the maximum and minimum values to normalize the attenuation measurement removes the impact of variations in LED intensity, PD performance, and path length variations [6, p.49].

Since pulse oximetry has traditionally focused on determining blood oxygen saturation (2.1), only two wavelengths of light have been used. Commonly selected in the red (R) and infrared regions (IR), these two wavelengths are chosen because Hb and HbO₂ exhibit different absorption characteristics in these regions, making it possible to distinguish their individual absorptions [6, p.46]. Since SpO₂ is only based on Hb and HbO₂ concentrations, the attenuations in the red and infrared can be used to find a “ratio of ratios” (2.2) that is directly related to the oxygen saturation [6, p.130].

$$SpO_2 = \frac{[HbO_2]}{[HbO_2] + [Hb]} \quad (2.1)$$

$$SpO_2 \approx R = \frac{\ln(I_{min,R}/I_{max,R})}{\ln(I_{min,IR}/I_{min,IR})} \quad (2.2)$$

The ratio R, is not itself the internal SpO₂ levels, but can empirically related to SpO₂. Typically this is done via calibration by inducing hypoxia in subjects and noting arterial SpO₂ and R values [8]. A drawback of using calibration is that only mild levels of hypoxia, down to 80%, can ethically be induced in subjects [6, p.160].

2.2.1 Measurement of COHb

From Beer’s Law, for n unknown concentrations in a substance, n different wavelengths and n extinction coefficients are required to resolve their individual

concentrations [6, p.42]. Typically, a pulse oximeter is designed to determine blood oxygen saturation (SpO_2), where only oxygenated hemoglobin (HbO_2) and reduced hemoglobin (Hb) concentrations are of interest. Needing only two concentrations, only two wavelengths are included in the design, typically at 660nm and 940nm [6, p.46].

However if carboxyhemoglobin is present, the SpO_2 type sensor will be unable to detect its presence, and will actually cause higher SpO_2 readings [6, p.160][9]. To expand the capabilities of the sensor, additional wavelengths are introduced to detect dysfunctional hemoglobins such as carboxyhemoglobin and methemoglobin. The blood saturations of carboxyhemoglobin and methemoglobin are SpCO and SpMET , respectively.

While it is only recently that commercial SpCO monitors have become available via the Masimo line of products [10], an early attempt to determine COHB was performed by Buinevicius [11] who used a three-wavelength oximeter to determine SpCO , however no validation testing of the results were presented. The current SpCO monitors from Masimo use eight different wavelengths and can detect carboxyhemoglobin and well as methemoglobin [12].

Overall devices monitoring SpO_2 and SpCO are technologically the same, they simply differ in the number of LEDs present.

2.3 Issues in Pulse Oximeter Design

2.3.1 Transmission and Reflective Oximeters

In order for an oximeter to function, light emitted from the LED must be able to pass through the vascular tissue and back to the PD. This can either be accomplished by transmitting light directly through the tissue to the PD, or by having the light reflect off a surface within the body and return to the PD. These

two types of configurations are known as transmission and reflective oximeters. While the configuration of the LED and PD are different, they are functionally the same [6, p.50].

Transmission pulse oximeters place the LED and PD on opposing sides of the tissue and measure the amount of light that passes through the area. To achieve this result, the area of interest must be relatively thin, such as the ear lobe [13], or fingertip [14]. Reflective oximeters position the LED and PD on the same side of the skin and measure the light that is reflected back to the detector. This design can be placed in a greater number of locations, including the forehead [15] [4], jaw [5] and finger[16].

Transmission pulse oximeters can only be placed in an area that is thin enough to permit light to pass through the body and to the photo detector. For a given design, the LED must be powerful enough such that the received signal is not too greatly attenuated by the other absorbers in the body such as skin pigment, bone, and venous blood [6, p.43]. If a measurement site is too thick, then the power of the LED must be increased, however skin irritation and burning are a concern [17, p.32].

For locations where a transmission pulse oximeter is infeasible, such as the chest or forehead, a reflective pulse oximeter can be used. A reflective oximeter can have a lower LED power consumption because the light does not need to pass through the tissue. However, the possibility of a direct optical path, or light short circuit, is another placement issue that needs to be considered. This issue occurs when the relative positions of the LED and PD move so close as to allow the light from the LED to directly reach the PD and corrupt the results [17, p.31].

There is no overriding issue that makes one configuration greater than another, thus the issue of selecting a configuration should be geared more towards

user comfort and availability.

2.3.2 Motion Artifacts

A key difficulty in deploying pulse oximetry for field applications is the interference of motion artifacts on the PPG signal. The calculations of the oximeter assume that the transmission medium is relatively constant, except for the pulsation of blood. If the LED and PD move relative to each other then the intensity varies not as a function of arterial blood, but of movement, corrupting the measurement.

To reduce motion artifacts, the sensor must be isolated from the source of motion. For a finger based sensor, Rhee *et al.* mechanically isolated the sensor from the external ring housing [16]. The motion of moving the hand, or its collision with an object was absorbed by the housing and reduced the impact on the sensor. Other attempts to remove motion artifacts have used signal processing algorithms such as the discrete saturation transform [18] [19], Fourier analysis [20], or accelerometer based adaptive filters [21] [22]. Related to our objectives, Comtios *et al.* [23] evaluated noise canceling algorithms for forehead based monitoring.

While many oximeter designs are “wearable”, few have been tested in real-life environments that would be required by a deployed product. Many designs have been tested while undergoing motion, however at times this motion is simply walking on a treadmill [24], shaking a hand [16], or a random tapping of the fingers [25]. More complex tasks have been performed by Johnston *et al.* [26] and Nagre *et al.* [5], that involved a helmet-based oximeter undergoing simulated military activities.

2.4 Review of Helmet-Based Oximetry

This study is not the first to integrate an oximeter into a helmet platform. Johnston *et al.* [26] and Nagre *et al.* [5] examined, forehead, jaw, and chin locations that were integrated into a military helmet. Furthermore, their tests involved complex motions such as talking, head movement, and riding in a vehicle. Following on that work, Dresher [4] [24] investigated the optimal pressure required to maintain a good PPG signal and also developed a fitted military helmet insert to allow proper blood flow.

While our project is similar in that an oximeter has been integrated into a construction helmet, the results of Johnston and Nagre are valid only for the military-type applications they tested and as such cannot be extended into the construction realm. Additionally, Dresher did not use real-time data, but spot checked his integrated sensor versus a finger based oximeter at various times during the testing.

While the tests employed by Dresher and Johnston validate their designs, their focus was on monitoring of soldiers where continuous measurement was of prime importance. Our study is different in that it does not seek continuous monitoring but a probable bound on performance based on the time to impairment by carbon monoxide. This study seeks to characterize the durations of motion artifact to ensure that they do not interfere with the overall objective of detecting CO poisoning. Relaxing the constraints of real-time monitoring is possible because construction workers will not be overcome from carbon monoxide instantly, but over a period of time.

Chapter 3

Methodology & Uptake

Estimation

This chapter overviews the methodology used to determine the feasibility of the integrated helmet-oximeter prototype. The helmet will be described as a repairable system in which motion artifacts of the user cause the helmet to fail and enter a repair state until the motion artifact passes, restoring the helmet to working order. In comparing the distribution of repair times to an estimate of time to impairment for a worker, the reliability of the helmet can be established. This chapter will outline the justification of the helmet as a repairable system as well as provide a derivation for worker time to impairment.

3.1 Determining Prototype Reliability

As the user moves throughout the workday so does the helmet and sensor. Based on how quickly or rapidly the user moves, the sensor may be disturbed to the point that it is unable to provide a reading. These periods where the sensor

cannot determine a person’s carbon monoxide levels cause “gaps” in monitoring. If these gaps are too long in duration, they may inhibit readings such that signs of a worker becoming affected are hidden. Thus, to prove the feasibility of the helmet, we must show that long gaps occur with such a small probability that the safety of the worker is not compromised. An example of measurement gaps are shown in Figure 3.1 with the gaps highlighted in red. The PPG signal is clearly distorted during the three gaps caused by the user hammering.

In answering this question we must first determine two things: (1) for an exposed population, what are the worst-case times to become impaired in the presence of carbon monoxide and (2) knowing this limit, what models can we use to find the probability of gap lengths longer those worst case times? The following sections outline the analytical methods required to find a probabilistic model of gap times and the analysis for determining time to impairment will be conducted in Section 3.3.

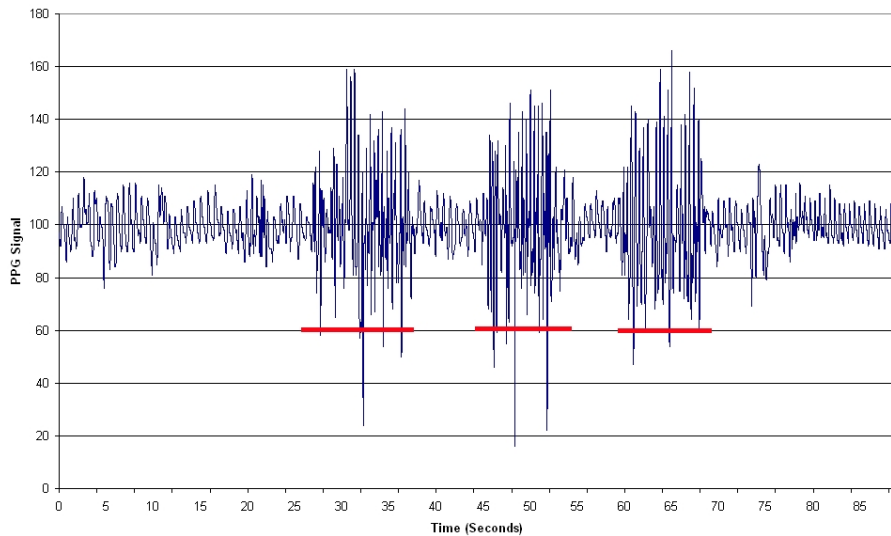


Figure 3.1: Measurement Gaps Induced by Hammering

3.2 Probabilistic Model of Sensor Performance

As this is the first study that seeks to characterize motion and measurement errors there is no existing work to help determine which probability distribution to choose when modeling the gaps. Thus our problem must be translated into a known form where analytical methods are already established. To accomplish this, the prototype’s performance will be moved into the context of a repairable system which is common in reliability analysis [27]. From there, existing tools and methods can be used to understand how the gaps are distributed.

The repairable system model characterizes the state of a device as either functional or non-functional. The time during which the device is working properly is called *uptime*. Because we are assuming a repairable system, when the system fails it immediately begins *repair time* and upon completing repairs is restored to *uptime* [27, p.85]. For our prototype helmet, the times at which the helmet is giving proper readings will be considered uptime, and once a measurement gap begins, the sensor will fail and be in repair time until a new valid measurement is received. The transition between these states is known because the oximeter transmits warning flags and indicators to identify the quality of the measurement. Specifically, we will assume any reading is a valid measurement unless one of the following conditions is met:

1. The presence of a warning flag indicating either out of track pulses, or the sensor is disconnected.
2. A “missing data” value is reported for SpO₂ or Heart Rate.
3. Reported SpO₂ is <95%.

Conditions (1) and (2) indicate normal functionality of the oximeter while (3) is a special case required due to ambient light contaminating the readings. It was found that during certain activities the helmet would report SpO₂ values

but because of the noisy signal, its values were obviously incorrect. In most cases the reported SpO₂ would drop below 90% during heavy motion, which is not correct considering a user would be experiencing a serious health event at that level and no users were under strenuous exercise. A level of 95% approximates a typical oxygen saturation value.

3.2.1 Gap Conditions

Using these conditions, the acquired readings can be partitioned into sequences of uptimes and repair times, where the repair times can be mapped into the lognormal distribution. This distribution is chosen because it is a common model for failure/repair times [27, p.94]. In previous works, Ananda [28][29] used a 2-parameter lognormal distribution for repair times while examining steady-state availability of systems. Schroeder and Gibson [30] examined several distributions to model high performance computing failures, finding that repair times were best modeled by a lognormal distribution. Also, software failure rates have been proposed to be distributed lognormally [31], and normal temperature distributions can cause lognormal failure rates in thin film conductors [32].

It must be noted that at times there exists a difficulty in selecting between the lognormal and Weibull distributions when modeling system lifetimes. The main concern is the impact of heavily tailed data, which is important in long range projections [33]. Realizing this concern, Chapter 5 shows that the lognormal distribution can be accepted under χ^2 goodness of fit analysis, whereas the Weibull cannot.

Finally, with the measurement gaps translated into the repairable system model, and the lognormal distribution selected to estimate gap events, we have the proper analytical tools to analyze the gaps. What remains is to find a proper estimate for time to impairment for the construction population. The analysis

to determine the impairment time is explained in the following sections and once having that estimate, the feasibility of the prototype will be shown in Chapter 5.

3.3 Prediction of Carbon Monoxide Uptake

The CO uptake model developed by Coburn, Forester, and Kane [34] relates exogenous CO exposure and endogenous CO production, along with relevant physiological parameters to estimate the amount of CO bound with hemoglobin (COHb). This model is known as the CFK equation and has been extensively verified in several studies and renders an accurate assessment of CO uptake for various exposure levels, body sizes, and activity levels [35][36][37].

3.3.1 The CFK Equation

The CFK equation treats the human physiology as a two compartment system in which exogenous and endogenous concentrations of carbon monoxide are exchanged by passing through the lungs. In a steady-state exposure environment, a person will gradually inhale and absorb carbon monoxide, producing carboxyhemoglobin, until an equilibrium with the outside environment has been produced. Because carbon monoxide diffuses equally in both directions, a person with a high internal concentration of COHb will naturally exhale the toxin if placed in an oxygen environment. The two compartmental model, combined with physiological parameters for respiration rate, and blood stores, are the basis of the CFK equation. The form given by Tikusis [37] is shown in (3.1).

$$\frac{d[COHb]}{dt} = \frac{V_{CO}}{V_B} + \frac{1}{V_B\beta} (P_{I_{CO}} - \frac{[COHb]P_{CO_2}}{[HbO_2]M}) \quad (3.1)$$

Additionally, (3.2) exists because CO binds with hemoglobin (Hb) in place

of oxygen, decreasing the amount of HbO_2 in the presence of COHb.

$$[HbO_2] = 1.38[Hb] - [COHb] \quad (3.2)$$

3.3.2 CFK Parameters and Units

While there are many parameters involving the CFK equation, many are either environmental or physiological constants that do not vary often. The complete table of parameters is shown below in Table 3.1. We will briefly distinguish between environmental parameters (P_{ICO} , P_L , P_{H_2O}) of which only P_{ICO} changes rapidly; physiological constants (D_L , M , P_{CO_2} , V_{co}) which remain stable; and physiological variables (V_B , V_A , $[HbO_2]$, $[COHb]$) which along with P_{ICO} are active in the determination of COHb levels.

Table 3.1: Parameters of the CFK Equation

V_{co} = endogenous CO production	V_B = blood volume (mL)
M = CO affinity for hemoglobin	P_{CO_2} = capillary pressure of O_2 (mmHg)
P_{ICO} = inspired pressure of CO (mmHg)	P_B = barometric pressure (mmHg)
V_A = alveolar ventilation rate	P_{H_2O} = vapor pressure of water (mmHg)
$[COHb]$ = CO concentration (g/mL)	$[HbO_2]$ = O_2 concentration (g/mL)
D_L = lung diffusivity (mL/(min*mmHg))	

Beyond having a large number of parameters to estimate, implementations and publications about the CFK equation suffer from differences between unit systems and translation of environmental factors between disciplines. Of critical importance is whether the values used in the solution come from Standard Temperature, Pressure Dry (STPD) or Body Temperature, Pressure Saturated (BTPS) systems. The main difference between the systems is whether water vapor is considered present in the lungs and at what temperature the exchange takes place. The original work by Coburn *et al.* used STPD, later validations

by Peterson *et al.* [36] used BTPS and Bernard *et al.* [35] returned to STPD. While values in either unit system can be translated between the other, the inconsistencies provide difficulty for initial studies. These discrepancies between unit systems is discussed extensively by Tikuisis [37].

Related to the above unit system differences, there exists a difficulty when comparing inhaled carbon monoxide measurements between fields. Where CFK uses the partial pressure of CO, P_{ICO} , the more common industry standard for toxins and pollutants are noted in parts per million (ppm). Often omitted in publications, the proper relationship between P_{ICO} and ppm is shown below.

$$P_{ICO} = \frac{ppmCO}{10^6}(P_B - P_{H_2O}) \quad (3.3)$$

Another difficulty in understanding CFK equation is that the final result, [COHb], is not the commonly used values of % COHB saturation. To convert from concentration in blood, to percentage saturation in blood use equation below (3.4):

$$\% \text{ COHb Saturation} = \frac{100 * [COHb]}{1.38 * [Hb]} \quad (3.4)$$

3.3.3 Solutions to CFK

Complexity is added to solving the CFK equation because [HbO2] is not constant but dependent on the current amount of [COHb] as defined in (3.2), thus the equation becomes non-linear and must be solved through numerical means. This relationship is a key point and is easy to miss when attempting a direct solution.

To compensate for this non-linearity, Peterson *et al.* [36] used a trial and error method to converge on the proper value of [COHb], whereas numerical integration with RK4 was used by Bernard *et al.* [35] and Tikuisis *et al.* [37]

with a small enough step size such that (3.2) could be updated at each step. Both methods were implemented in this work and little difference was noted between the two solutions. With RK4 a more commonly known and accepted method, it will be our used for our analysis. During simulation a step size of .01 minutes was used.

3.4 Determination of Worker Profile

To understand what level of coverage is required by the worker population, we must understand what factors effect carbon monoxide uptake the most. Looking at (3.1), this is not directly obvious, but when considering how CO enters, exits, and binds to the body the most important variables are clear. The build up of carbon monoxide within the body is directly related to how much is inhaled, exhaled, and how rapidly over that time period. The faster a person breathes the quicker CO will diffuse across the lungs. In cases of poisoning, when two equivalent people are exposed, the person who is breathing the most or working hardest will present advanced symptoms quicker, revealing that V_A is key in CO uptake.

Because of (3.2) the effects of CO poisoning become more severe as COHb increases relative to total blood count, thus those with high CO background levels, low hemoglobin counts, or small body size are at significantly greater risk when doing equivalent work. Thus if two people are working at the same activity level, in the same exposure level, the one who is already a smoker, smaller, or suffering from anemia, will be overcome in a much shorter timespan. By this understanding, background Hb and V_B values greatly influence the uptake of CO.

To measure how these variable affect a population, two profiles were created for typical and at-risk workers with each profile working at resting, moderate,

and intense levels of activity. The two theoretical subjects were exposed at an extremely high concentration of 1,200 ppm which is defined as Immediate Danger to Life and Health by NIOSH [7, p.3]. Recognizing the impact of activity level, resting, moderate and intense levels of activity were derived from exercise conditions in [38, p.269]. The physiological profile of both workers is shown in Table 3.2. Additionally, the at-risk worker was considered to be anemic as defined by the World Health Organization [39, p.4]. This is an especially important condition as 30% of men in non-industrial countries are anemic [40, p.15]. Also, each worker is given a high background level of carboxyhemoglobin as if they were smokers.

The values selected for the at-risk worker are intentionally chosen to setup a worst-case estimate. In setting up this hard limit, if the helmet is able to sufficiently monitor these worst-case workers, then it will be able to monitor healthier workers as well.

Table 3.2: Profile of Typical and At-Risk Workers

Physiological Parameters	Typical	At-Risk
V_B (mL) [36]	5,500	5,000
[Hb] (g/100mL) [39]	15.71	13.0
Initial COHb (% Saturation)	5	5

Table 3.3: Respiratory Exercise Parameters for Various Intensities

	V_T (mL)	f	V_D (mL)	\dot{V}_A (mL)
Resting	500	12	200	3600
Moderate	2,500	30	150	70,500
Intense	3,000	50	150	142,500

The various levels of activity were derived from tidal volume (V_T), dead space (V_D), and breaths per minute (f) values given in [38] and converted to

\dot{V}_A measurements by (3.5). The resulting activity levels are shown in Table 3.3.

$$\dot{V}_A = f(V_T - V_D) \tag{3.5}$$

3.5 Time to Impairment and Incapacitation

A carboxyhemoglobin saturation at 30% results in confusion and impairment, whereas at 60% a person would become unconscious and eventually die if not rescued [3]. Our approach is similar to that of Alari [41] and Bernard and Duker [35] who used the CFK equation to model escape times from fires. Also, Tikuisis compared theoretical and measured values of COHB for resting [42] and exercising subjects [43].

The two worker profiles were estimated at the activity levels shown in Table 3.3, the results of the estimation are shown in Table 3.4 and Figure 3.2 provides a graphical representation for the uptake curves.

Table 3.4: Time to Impairment (30% COHb) and Incapacitation (60% COHb) in Minutes at 1200 ppm

	Resting (30/60%)		Moderate (30/60%)		Intense (30/60%)	
Typical	97.0	300.2	17.5	57.0	15.5	50.4
Anemic	69.2	225.8	13.1	42.9	11.6	37.9

Viewing Table 3.4, the impact of higher activity levels and lower red blood cell counts is revealed by the faster times to impairment and incapacitation.

Returning to the definitions of worst-case time to impairment (T_i), Table 3.4 provides these values. As would be expected, the worst-case overall is the worker that is both anemic and performing intense activity. For this particular worker $T_i=11.6$. It is these bounds at which the prototype will be tested against to determine if it sufficiently covers the worker population.

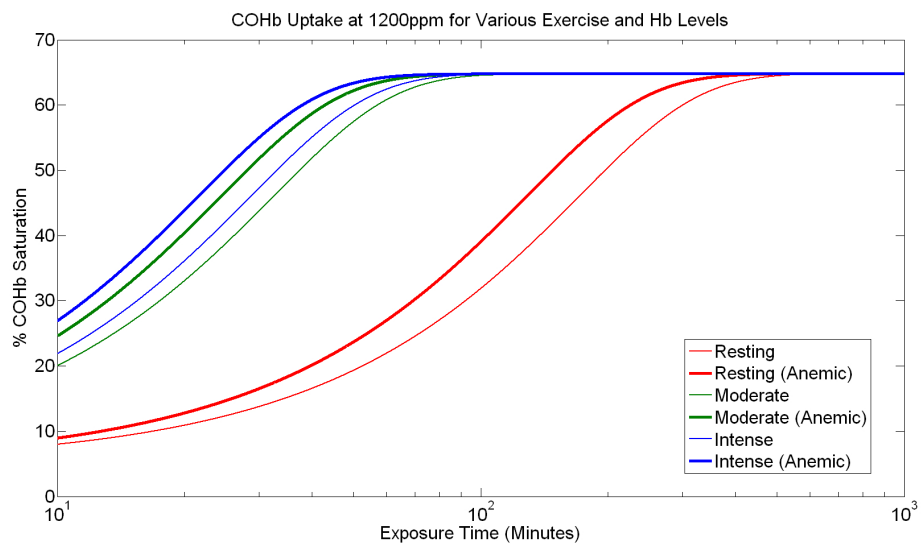


Figure 3.2: Carbon Monoxide Uptake at 1200ppm

Chapter 4

Prototype Development & User Study

This chapter provides an overview of design and construction of the integrated helmet prototype as well as the user study conducted to validate the design. We will describe the physiological and wearability requirements that were a driving force in the design. Additionally, we will outline the required substitution of the CO pulse oximeter for a traditional blood oxygen oximeter.

4.1 Physiological & Wearability Requirements

In designing for the construction worker population it is of prime importance to have a device that is not only functional but is extremely non-intrusive to their daily lives. Even if the workers are convinced of the criticality of monitoring for CO, if the device gets in the way of their accustomed activities and encumbers their work, they are unlikely to take to the device.

Thus a method of integration must be found that is both physiologically

acceptable for monitoring, but also culturally, aesthetically, and functionally desirable for the worker. To begin, there are several possible sites on the body that have shown to be acceptable monitoring locations for pulse oximetry including the finger, wrist, earlobe, forehead, and facial regions. Table 4.1 shows various comparative studies of sensor placements that have been conducted. Indicated are: the types of sensors compared, where [R] denotes a reflective sensor and [T] denotes a transmission; whether the subjects were in motion or at rest; and which measurement site provided the best result.

Table 4.1: Comparison of Various Sensor Placements

Author	Locations Compared	Motion	Preferred Site
Mendelson <i>et al</i> [44]	forehead[R], finger[T]	N	forehead
Mendelson & Pujary [45]	forehead[R], wrist[R]	N	forehead
Narge & Mendelson [5]	forehead[R], finger tip[T], jaw[R], chin[R]	Y	forehead
Nogawa <i>et al</i> [46]	forehead[R], chest[R]	N	forehead
Rhee <i>et al</i> [16]	fingertip[T], finger[R]	Y	finger

4.1.1 Wrist & Finger

Now let us consider the impact of various monitoring sites on the ability and dexterity of the worker. The finger and fingertip has long been the traditional measurement location of pulse oximetry with one of the first truly wearable designs by Rhee [47] being a large ring where the oximeter was housed. Furthermore, measuring from the fingertip is very common in hospital settings and many medical devices use this location [14] [10]. However, these designs are very

restrictive to the dexterity of the worker with each design covering a significant portion of the finger. Considering the target population works closely with hand tools, it is unlikely that any design encumbering the hands will be accepted.

Additionally, while a wrist based sensor has been attempted [45][48], the complex bone structure in the wrist does not lend itself to being a stable location for light back scattering that is required in reflective oximeters. While plausible, no studies have shown the wrist to be a reliable location.

4.1.2 Facial Regions

Several studies have examined regions of the face for possible oximetry monitoring including the forehead, jaw, and chin [5][26]. It was noted that during motion or even talking, the jaw and chin sensors would be unusable due to motion [26, p.215]. When undergoing combat simulation exercises, the forehead sensor was found to be less affected by motion than chin or jaw sensors [5, p.2].

While early oximeter designs also used the ear as a potential location [6, p.33][15, p.800], development ready parts are not available for this location and will likely not be accepted by the worker. However a design could integrate the sensor within a common bluetooth ear piece, potentially making the device desirable to be worn. Designs similar to this have been conducted by Wang *et al* [13].

4.1.3 Selection of Forehead

Overall, the forehead is viewed as a good location for measurement as it is resistant to motion and has sufficient density of vascular elements to provide a reading. Additionally, the large bone structure is fairly regular and provides a simple background from which to capture reflected light. Beyond the physiological considerations, the forehead is a prime location because it does not

affect the dexterity of the user and can also be easily integrated into existing headwear, such as the military helmet integration performed by Dresher [4].

4.2 Substitution of SpCO for SpO₂

Ideally, in investigating a wearable solution for monitoring carbon monoxide, the Masimo [10] line of products would be modified to become a wearable device. However, this route is not possible due to two particular reasons. First, the Masimo products are prohibitively expensive for this project and it would not be cost effective to modify their products. Second, the algorithms and signal processing methods used to detect SpCO are proprietary and it is not guaranteed that modifying their sensors would result in proper functionality.

A solution can be found by understanding the equivalent methods used between SpO₂ and SpCO measurement. Both techniques follow the same principles of pulse oximetry, the comparison of emitted and received light through vascular tissue. However the Masimo technology simply increases the number of wavelengths used to determine additional blood components. This follows directly from their patent filings where additional wavelengths are used to determine hemocrit, carboxyhemoglobin, and methhemoglobin (U.S. Patent 7,274,955). Furthermore, the similarity between SpO₂ and SpCO systems is shown in a three-wavelength oximeter developed by Buinevicius where an additional LED at 810nm was added to the traditional LEDs to account for the presence of carbon monoxide [11].

With an equivalent method for measuring SpO₂ and SpCO, traditional pulse oximeters can be substituted for a SpCO oximeter for design and testing purposes. While they do not provide the same measurements, the substitution allows for adequate approximation of wearability, physiological feasibility, and energy constraints with the added benefit of using a well developed and inex-

pensive technology.

4.3 Helmet Prototype

In order to avoid developing our own oximeter, we selected the Xpod pulse oximetry from Nonin [49] utilizing a reflective sensor attachment. Marketed as an easy to use development kit, the Xpod is frequently used in prototypes that monitor from the forehead [4][45][5][26][50]. To enable wireless transmission of readings, the output of the Xpod was connected to an Xbee Radio from Digi Inc. [51] that transmits the readings of the Xpod to an Xbee base station connected to a laptop. The Xbee radios communicate using the Zigbee protocol.

The final prototype is shown in Figure 4.1, with the interior view showing the attached Xpod and sensor integrated into the headband. The back view shows the Xpod connection to the Xbee and required 9V battery. The following sections describe the design implications that lead to the prototype's final form. In general, the design process was driven by a desire to shape the internal headband such that it minimized motion artifacts, and to place the electronics to reduce the impact of their weight.

4.4 Headband Design

The headband insert shown in Figure 4.1a was not the final form factor selected for the user study. An earlier design did not have the sensor surrounded by the foam insert, causing the sensor to easily slip out of place when the helmet was removed. The current design is a vinyl front with a foam backing that attaches to the natural helmet headband by Velcro. The sensor is recessed into the headband such that it is pressed against the forehead, but the extra foam padding softens the design and provides even pressure across the forehead. The

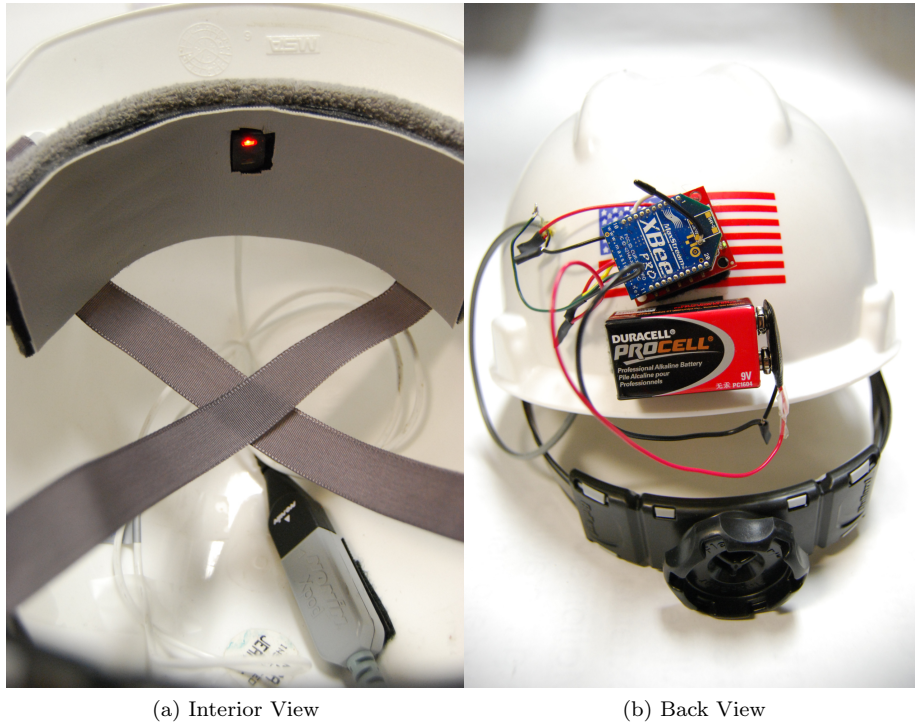


Figure 4.1: Interior and Back of Helmet Prototype

recessed sensor and foam insert are shown in detail in Figure 4.2.

4.4.1 Motion Issues

The final design was a compromise between comfort and the desire to reduce motion artifacts, the main obstacle in helmet based monitoring. Since a reflective oximeter is required for use on the forehead, the sensor must remain still such that the backscattering reflections off the frontal bone are consistent over time. If the sensor moves relative to the forehead, motion errors are induced and a reading may not be possible. For reference, a normal PPG signal from the helmet prototype is shown in Figure 4.3a. In moving the helmet side to side, as if to say “No”, slight motion errors are induced in Figure 4.3b. However in

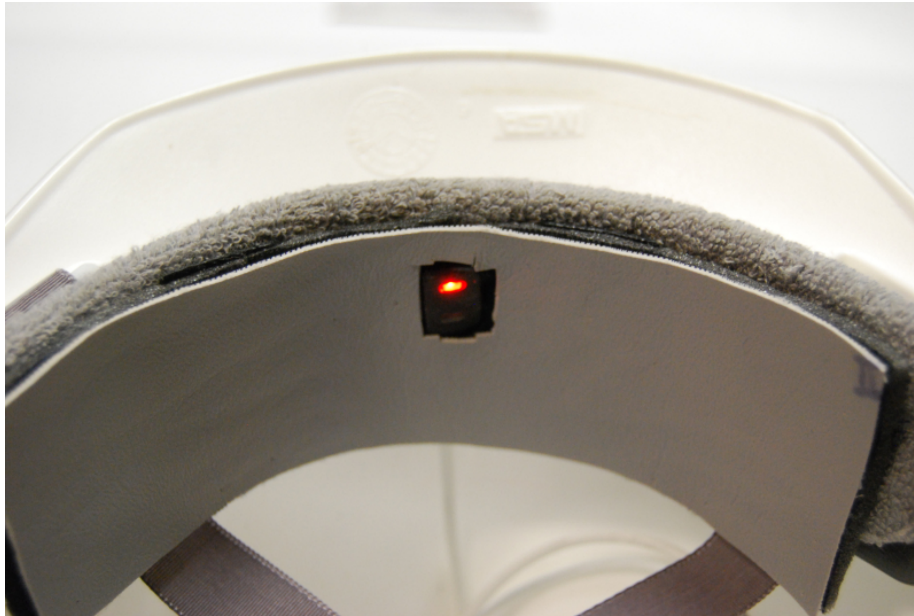


Figure 4.2: Modified Helmet Headband

Figure 4.3c, moving the helmet up and down, as if to say “Yes”, induces major errors and the signal becomes unusable. A major cause of motion is the torque moment applied by the helmet to the sensor. Because the sensor is physically integrated into the helmet, as it moves, so does the sensor and depending on the amplitude and frequency of movement, no measurement may be possible.

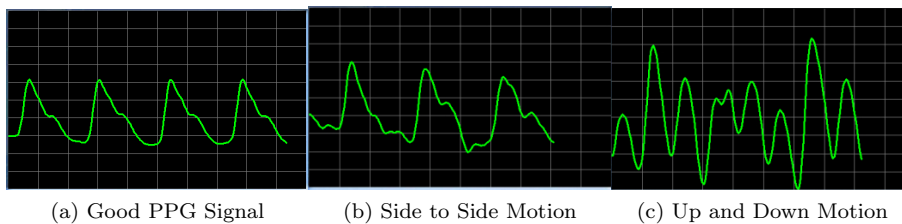


Figure 4.3: Motion Induced Errors in PPG

Several design iterations were conducted that attempted to isolate the sensor from the helmet. Overall these attempts were unsuccessful because specific

pressure is required at a location to hold the sensor in place. This singular pressure point is extremely uncomfortable given that during typical wear the headband pressure is distributed evenly across the forehead. The best possible solution would be to mechanically isolate the internal assembly from the outer protective shell of the helmet. This strategy was used by Rhee when he separated the internal sensors closest to the finger from the outer metal shell with only thin wires connecting the two [16]. Applying this method to the helmet, the internal assembly could be a simple elastic headband to which the sensor is integrated. The outer hard part of the helmet would still be attached, but in such a way that it moves freely apart from the headband, much like the independent sections of a gyroscope. It is unknown whether a design of this type would meet the required safety standards, but the potentiality of a reliable helmet design is worthy of further study.

4.5 Electronics & Placement

As briefly mentioned, the final prototype includes three major electronic components: the Xpod oximeter, the Xbee Zigbee radio, and a 9V battery for power. The electrical and communication connections between the devices are shown in Figure 4.4.

4.5.1 Communication & Power

The main connection point in the design is the break out board which holds the Xbee module. This board, purchased from SparkFun [52], allows direct access to the Xbee pins and provides a regulator that steps down the 9V battery output to 3.3V which supplies operating power for both the Xbee and the Xpod.

The primary reason for using the Xbee is simplicity. In its most basic configuration the device acts as a UART replacement, transmitting over the radio

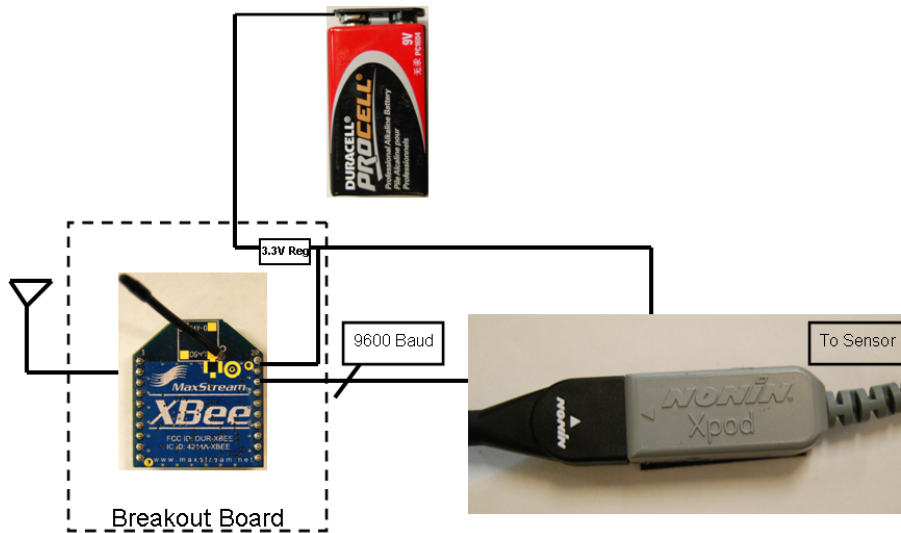


Figure 4.4: Schematic of Prototype Components

items it receives via UART and sending across its UART the packets received on the radio. In this manner, the Xpod can easily be made into a wireless device by connecting its output line directly to the Xbee. The measurements from the Xpod are transmitted 75 times a second at 9600 baud to the Xbee where it is broadcast to another Xbee base station. This base station is connected to a laptop via USB virtual serial port, from which the native Nonin Oximetry software can read the Xpod’s measurements and run without modification.

While indoor ranges of 30 meters are listed for the Xbee modules, in cluttered environment these ranges were not possible unless a higher-gain antenna was used at the base station. Initially the “whip” type antenna used on the helmet was at both locations. However in this configuration data was dropped after only 5 meters. Replacing the whip antenna on the basestation with the U.F.L type antenna in Figure 4.5 resolved the problem with only a handful of packet being dropped.

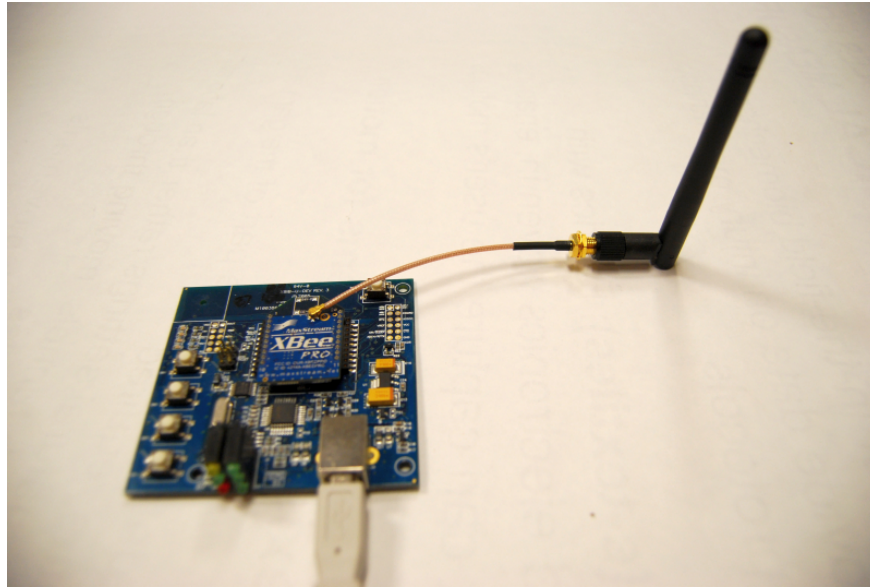


Figure 4.5: High Gain Xbee Antenna

4.5.2 Energy Consumption

During testing, the lifetime of the prototype was only several hours, where a lifetime of several days would be required from a final product. During operation, the entire prototype consumes 91mA which is constant because of the linear regulator. With the Xpod consuming 18 mA, the main power draw of the prototype is the Xbee radio. The Xbee consumes 55 mA while idle or receiving and 250 mA during transmission. Since the system is not transmitting continuously, the total current draw of the radio is less, resulting in the 91mA total current draw.

In a deployed system, monitoring of the worker would be localized and power consumptions could be much less. To enable local monitoring, a small microcontroller would need to be added to the system to monitor the oximetry readings. The Xbee radio would remain but would only be activated in case of an emergency where an alert was required. The lifetimes of these two systems when

running on a typical alkaline [53] and lithium 9V battery [54] are compared in Table 4.2. The microcontroller on the future deployed system is estimated with a PIC18 [55]. Additionally, different types of power regulators are shown with the linear regulator lifetimes shown directly, and the switching regulation lifetimes shown in parenthesis. The switching regulator was assumed to be 95% efficient.

Table 4.2: System Lifetimes in Hours of Current and Future Deployed Designs for Linear and Switching Regulators

Design	Components	I_{nom}	P_{nom}	9V Alkaline	9V Lithium
Prototype	Xpod, XBee	91mA	303mW	6h (15h)	8h (20h)
Deployed	Xpod, XBee, PIC18	26.1mA	86mW	21h (54h)	29h (76h)

The system lifetime estimates were derived as follows. For a linear regulator, such as the one presently used, the system lifetime L_{linear} can be found from equation (4.1) where C_{nom} and I_{nom} are the nominal battery charge capacity and nominal current draw, respectively. For a switching regulator, the system lifetime L_{switch} are given by equation (4.2) where V_{nom} and the P_{nom} are the nominal battery voltage and nominal system power, respectively.

$$L_{linear} \approx \frac{C_{nom}}{I_{nom}} \quad (4.1)$$

$$L_{switch} \approx \frac{V_{nom}C_{nom}}{P_{nom}} \quad (4.2)$$

In both equations, the charge capacity of the battery is required. However, the charge capacity offered by the battery changes over time based on load and current draws. The information provided by the manufacturer in [53] [54] does not allow for the charge capacity to be known at all times. To be fair in comparisons, for each battery type we used a nominal capacity that is the

average capacity at a constant draw of 25mA and 100mA, which are the closest values to our two potential systems. The derived nominal capacity for the alkaline and lithium batteries are 550mAh and 762mAh, respectively.

As the results in Table 4.2 show, removing the Xbee radio from an active role in the design greatly increases the expected battery life. Additionally, power is wasted by the linear regulator in dropping the supply voltage from 9V to 3.3V. The 9V battery and connector were original to the Xpod and for simplicity they were kept in the design. Recognizing that the design can run at 3.3V, a supply closer to that threshold would provide better efficiency and longer lifetimes.

4.5.3 Placement Considerations

Initially the Xpod was placed on the brim of the helmet, but the additional weight, was quickly noticed as a tilting force to the helmet. By relocating the Xpod to the interior, the device is not noticed by the user. A production version of the helmet should consider the weight distribution of the electronics to reduce the effects of the weight on the movement on the helmet.

4.6 User Study

A user study was conducted to validate the helmet prototype design. The study featured ten students performing six construction related tasks intended to mimic typical motions and actions of construction workers. The study was conducted in Torgersen Hall on the campus of Virginia Tech and was approved by the Virginia Tech Internal Review Board (IRB # 09-768).

4.6.1 Selection of Tasks

Six individual tasks were selected for the user study and were performed over two weeks by the students. Each task sought to mimic the activities and motions of a construction worker without necessarily the impact or stress that performing the actual activity would cause. No standardized set of safety activities or motions was found, however the selected activities were deemed sufficient for our purposes. While none of the activities are as intensive in action and duration as some construction tasks, this distinction was intentional because of the nature of the study. As this is an initial study, if the helmet cannot pass the simple tasks presented here, then it will not pass more rigorous ones later.

4.6.2 Selection of Participants

Study participants were fellow graduate and undergraduate students who knew about the project during its development. Experienced workers in construction are not required because only the motions of tasks need to be approximated, not necessarily the task itself. A person does not need to be an expert hammerer to approximate the required hammering motion. Likewise, for the simple tasks selected, moving boxes, walking, or sweeping the inherent motions are assumed to be equivalent between experienced and non-experienced users.

4.6.3 Walking and Stairs

After placing the helmet on the user and acquiring a good reading, each user was instructed to walk around the third floor of Torgersen three times. This task is a baseline measurement of helmet performance; if the motion of walking is too great, then more advanced tasks are not feasible. After completing the walking circuit, the users were asked to walk down the stairs to the first floor twice and then return. Figures 4.6a and 4.6b show the third floor of Torgersen

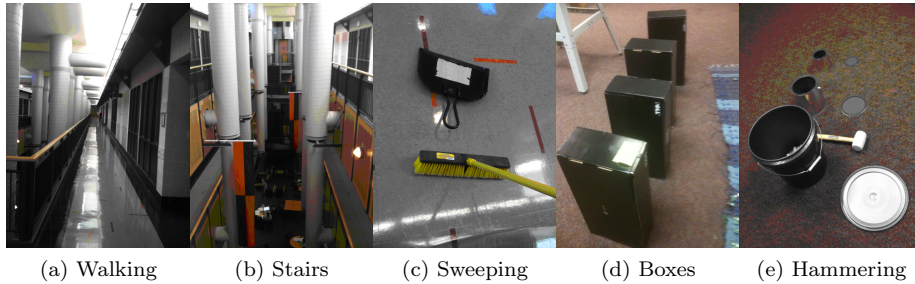


Figure 4.6: User Study Activities

where these two tasks occurred.

4.6.4 Sweeping

A more involved motion was desired to ascertain the effects of upper body movement on the helmet. To approximate this motion, many pieces of paper were dumped on the floor in Torgersen Hall and the user was asked to sweep up these items, this task was repeated three times. The user was not idle while performing this task and had to move around and sweep to complete the activity.

4.6.5 Hammering and Boxes

The final tasks were to have the users hammer on several paint cans and move boxes around a laboratory. These acts simulate the effects of hand tools on head motion and also the bending and lifting motions of carrying. Hammering was conducted with the cans both on the floor and on a saw horse. For the boxes task, each boxes was individually labeled and the users were asked to move them across a room and stack them in proper order. This task involved multiple motions of moving, bending, and lifting to accomplish.

Chapter 5

Results

This chapter presents the results of the user study and highlights the overall performance of the prototype and contributing factors that determined the quality of measurements.

5.1 Validating Helmet Reliability

As outlined in Chapter 3, the validity of the helmet prototype is predicated on its ability to warn the worker before he or she becomes impaired from carbon monoxide exposure. The user study provides sensor data which can be used to determine how reliably the prototype operates during construction activities. Because this type of study has not been conducted before, simple tasks were specifically selected such that if the helmet could not perform these items easily, then it would not be able to perform more rigorous tasks that would be required for a complete safety device.

The data from the study was broken down into sequences of measurement gaps, as defined in Section 3.2.1. The distribution of these gaps is critical to understanding the safety of the helmet. The observed distribution of gaps is

shown in Figure 5.1. The x-axis describes the gap length in seconds and the y-axis reveals the observed frequency of each gap occurring.

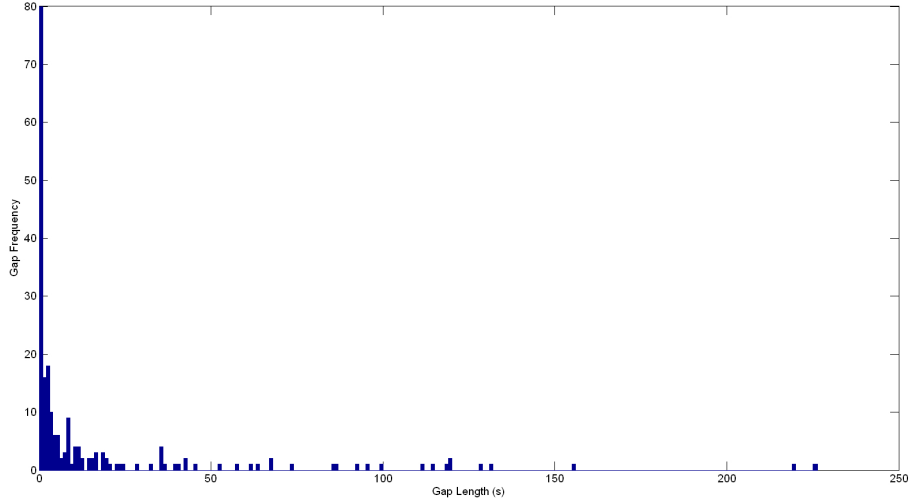


Figure 5.1: Distribution of Gaps from User Study

To have a reliable system we want to avoid long gaps in measurement. It is a welcome sign that a majority of gaps are short in duration, indicated by high frequencies near the y-axis. Recalling the work in Chapter 3, we are interested in knowing the probability of gaps (X) above a time to impairment threshold (T_i minutes). This probability can be expressed by equation (5.1).

$$P(X \geq T_i) \tag{5.1}$$

Replacing P with the lognormal distribution, we can rewrite (5.1) as (5.2) where F is the lognormal cumulative distribution function. The parameters μ and σ are the shape parameters for the lognormal.

$$P(X \geq T_i) = 1 - F(T_i|\mu, \sigma) \tag{5.2}$$

We can fit the lognormal distribution to the observed gaps with the MAT-

LAB command *lognfit*, which returns estimates at $\mu = 1.0155$ and $\sigma = 2.0256$. Illustrated in Figure 5.2, this new estimated distribution closely fits the plot of observed gaps.

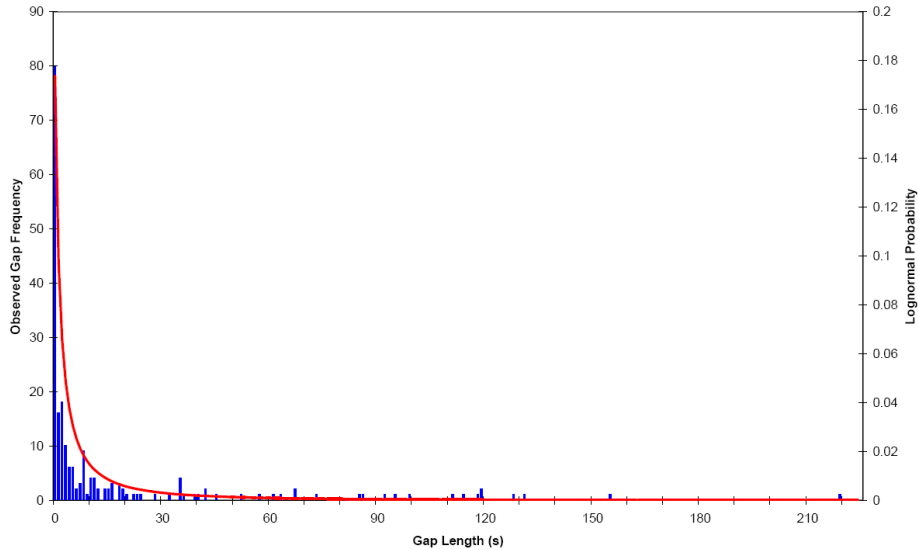


Figure 5.2: Histogram Fitted with Lognormal Distribution

With the estimates of μ and σ along with value of T_i , we can directly find the probability of a gap occurring that is longer than T_i . Solving (5.2), the probability of such an event is $p = 0.0034$. (T_i , which is in minutes, must be multiplied by 60 to convert into seconds.)

$$P(X \geq T_i) = 1 - F(11 * 60 | 1.0155, 2.0265) = 0.0034 \quad (5.3)$$

Equation (5.3) reveals how likely the prototype is to fail while monitoring a worker. Conversely, the probability the helmet will adequately protect the worker is $1-p$, or 99.66%.

While this is an excellent result, given the way our gap objective is constructed, it is possible a single measurement could occur near time zero and then the remaining time to T_i could be covered by a gap. This situation would

still be considered valid monitoring time, as the gap would not be the full length of T_i . However, depending on how early the singular measurement occurs, it may not contain any useful information as internal carbon monoxide levels may not have risen to the level of concern.

To counter this possibility, we can divide T_i in half to create two new measurement intervals against which we will test the probability of measurement gaps. While early measurements in the domain $[0-T_i/2]$ may not reveal any carbon monoxide presence, at $T_i/2$ the internal levels for our worst-case worker will be 17.5%. Thus any measurement in $[T_i/2 - T_i]$ will warn of the presence of CO. Replacing T_i with $T_i/2$ in equation (5.2), we find the the probability of a gap covering the new $T_i/2$ intervals is $p = 0.0091$ or 0.91%. Conversely, this indicates the helmet will provide protect the worker with probability 99.09% in these new restrictive intervals, giving a strong indication that the helmet will find a valid reading upon which to act and accurately warn the worker.

Regarding the probabilities derived above, a point can be made that the probability of a gap occurring near T_i will be low because none of the activities in the study were long enough to create gaps of length T_i . While this is a valid point, if significant measurement outages were frequent, the distribution of gaps in Figure 5.1 would not be so closely aligned to the y-axis; the addition of more long duration gaps would be unlikely to shift the curve. Furthermore, we do not assert that the probability of large gaps is zero. In fact it is quite easy to construct activities where no measurement is even possible. However with these basic, but reasonable tasks, we have shown that it is feasible to conduct monitoring during typical construction tasks. Further work in isolating the sensor from helmet motion, and longer, more complex tasks will allow a greater understanding of the true abilities of the prototype. Yet as a proof-of-concept, the helmet verifies the idea of an integrated pulse oximeter for construction

activities. Moreover, because of the criticality of the monitoring construction workers, even results that show feasibility demand further study.

5.1.1 Choice of Distribution

As briefly mentioned in Section 3.2, at times there is an ambiguity between selecting the lognormal or Weibull distribution [33]. The main concern is the impact of heavily tailed data on the overall result. To determine the correctness of our selection, Table 5.1 shows the estimations of $P(X \geq T_i)$ for the lognormal and Weibull distributions.

Table 5.1: Metrics of Fit to Histogram

Distribution	$P(X \geq T_i/2)$	$P(X \geq T_i)$	χ^2 p-value
Lognormal	0.0091	0.0034	0.1785
Weibull	0.0013	$7.71E - 5$	0.0349

This concern is evident when comparing the gap probabilities at various points along the curve. At $T_i/2$, the probabilities are on the same order, however when extrapolating to T_i the difference becomes two orders of magnitude. We can be assured that the lognormal is the correct choice by the χ^2 p-value. At 5% significance, we can reject that the gaps come from a Weibull distribution, but cannot reject they are from a lognormal distribution. Furthermore, Figure 5.3 provides a visual indication of how well the distributions fit. The exponential distribution is also included because at times it is substituted for the lognormal for ease of computation [56].

5.2 Helmet Performance Factors

The previous section provides an understanding of how the helmet performed over the whole study; this section seeks to break down the data and understand

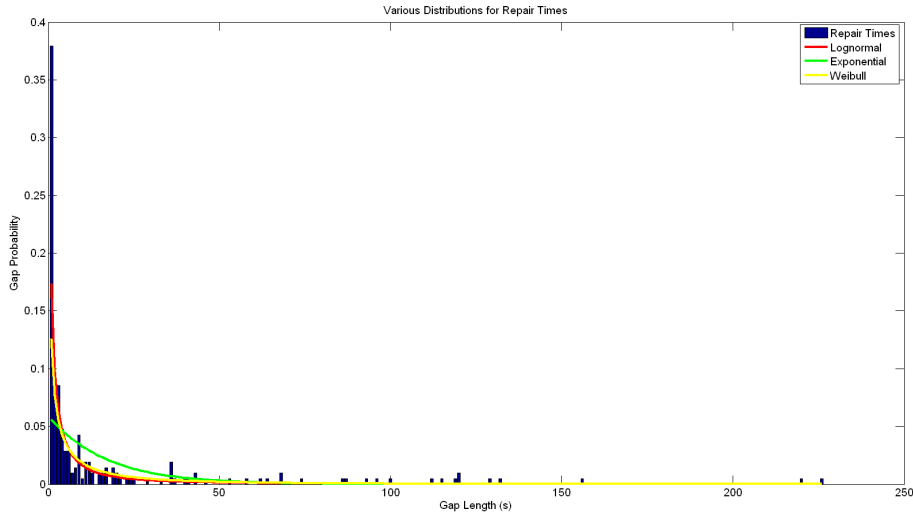


Figure 5.3: Various Distributions Mapped to Histogram

individual factors influenced the helmet. Table 5.2 shows the average, total, and maximum gap times for each user and activity. In general, the lower the total gap time, the more valid measurements the sensor was able to acquire. The total gap information is plotted in Figure 5.4. Also, Table 5.2 and Table 5.3 provides the amount of time taken by each user to perform each activity. The hammer and hammer2 activities differ in whether the hammer was performed on the ground, or on a sawhorse.

Table 5.2: User Performance: Average, Maximum, Total Gap in Seconds

User	Walking			Stairs			Sweeping		
U1	4.5	10.7	13.4	0.9	3.0	4.6	11.7	28.8	46.9
U2	4.0	11.6	31.7	0.6	2.0	3.9	42.1	57.1	126.3
U3	0.3	0.4	0.5	0.4	0.4	1.7	19.3	32.6	58.1
U4	0.0	0.0	0.0	2.3	3.8	9.5	23.2	37.0	116.0
U5	0.0	0.0	0.0	0.0	0.0	0.0	0.0	0.0	0.0
U6	5.4	19.8	42.9	31.8	85.3	95.4	117.4	226.3	234.8
U7	29.2	74.0	204.4	4.3	67.1	90.8	219.3	219.3	219.3
U8	0.2	0.5	0.5	38.7	99.9	116.3	0.0	0.0	0.0
U9	0.4	0.5	1.5	2.9	14.5	29.2	6.8	8.2	13.7
U10	2.7	42.5	67.1	44.0	131.1	132.0	58.8	155.8	176.4

Table 5.3: User Performance: Average, Maximum, Total Gap in Seconds

User	Boxes	Hammer	Hammer 2
U1	0.0 0.0 0.0	24.5 67.0 98.3	0.0 0.0 0.0
U2	22.8 61.1 114.3	43.2 46.0 86.4	95.8 95.8 95.8
U3	12.0 24.0 24.1	6.1 11.2 18.4	2.6 3.7 5.3
U4	3.4 9.0 10.2	40.2 93.0 120.8	10.7 16.3 53.6
U5	1.4 2.5 2.8	24.6 43.0 74.0	1.6 1.6 1.6
U6	60.3 119.8 120.7	29.5 118.0 147.9	42.1 114.5 126.3
U7	23.0 87.0 115.4	129.0 129.0 129.0	56.8 111.3 113.7
U8	0.2 0.2 0.2	0.0 0.0 0.0	0.0 0.0 0.0
U9	1.4 2.7 2.8	1.8 1.8 1.8	8.0 12.7 16.1
U10	14.9 35.1 59.6	42.1 119.3 126.3	9.3 10.3 28.0

Table 5.4: Activity Durations in Minutes for Each User

	Walking	Stairs	Sweeping	Boxes	Hammer	Hammer2
U1	3.96	2.83	3.06	2.81	2.51	2.36
U2	4.15	2.85	3.51	2.96	2.5	2.26
U3	5.18	2.95	4.03	1.81	2.25	2.98
U4	4.53	2.81	3.61	1.36	2.68	2.81
U5	4.1	2.7	3.63	1.76	2.41	2.43
U6	3.71	2.76	4.46	2.28	3.15	2.38
U7	4.71	3.9	4.75	3.28	2.63	2.46
U8	4.51	3.58	3.63	1.98	2.48	2.55
U9	4.38	2.83	4.66	3.45	2.41	2.33
U10	3.8	3	3.71	1.95	2.63	2.16

Total gap size is an aggregate measure that can tell how the helmet performed overall for particular user and activity. If the total gap is small, that implies the sensor was able to gather more valid readings during the activity. A key to understanding the helmet’s monitoring behavior is to determine which factor, Users or Activities, had a significant impact on the total gap size. Since User and Activities are the only two factors considered in the study, if we can show that one has equal effect, then the other must be the cause of variations in total gap size.

5.2.1 Activities and Total Gap Size

If we organize total gap information into a matrix of Users by Activities such as in Table 5.5, we can use Friedman’s Test to determine if the columns (Activities) have equal or non-equal effects on the total gap size. If the activity effects are equal, then we can conclude that user effects have a greater impact on the total gap size.

Table 5.5: Total Gap Organization for Friedman Analysis

	Walking	Stairs	Sweeping	Boxes	Hammer	Hammer2
U1
U2
U3
...

Using the MATLAB command, *friedman*, we can analyze the total gap data and either accept or reject the null hypothesis H_0 that all column effects are the same. The resulting analysis is shown in Table 5.6 where SS is Sum of Squares, df is degrees of freedom, and MS is Mean Squares. The p-value is found to be $p = 0.0708$, which at 5% significance indicates we cannot reject H_0 . This result confirms that the effects of all the Activities are statistically equal and the differences noticed in total gap size are a function of the Users.

Table 5.6: Results of Friedman’s Test

Source	SS	df	MS	χ^2	Prob> χ^2
Columns	34.55	5	6.91	10.16	0.0708
Error	134.45	45	3.01		
Total	170	59			

5.2.2 Users and Total Gap Size

Looking at Figure 5.4, there is a range in the quality of monitoring by the helmet over the several users. Grouping these users visually by thirds, we have Group I, where five users have a total gap time of less than 300 seconds, indicating a slight loss of monitoring; Group II, where three users have total gaps in the range of 300 to 600 seconds indicating a mild loss; and finally the helmet performed poorly with two users who have total gaps of over 600 seconds. These groupings are shown in Table 5.7.

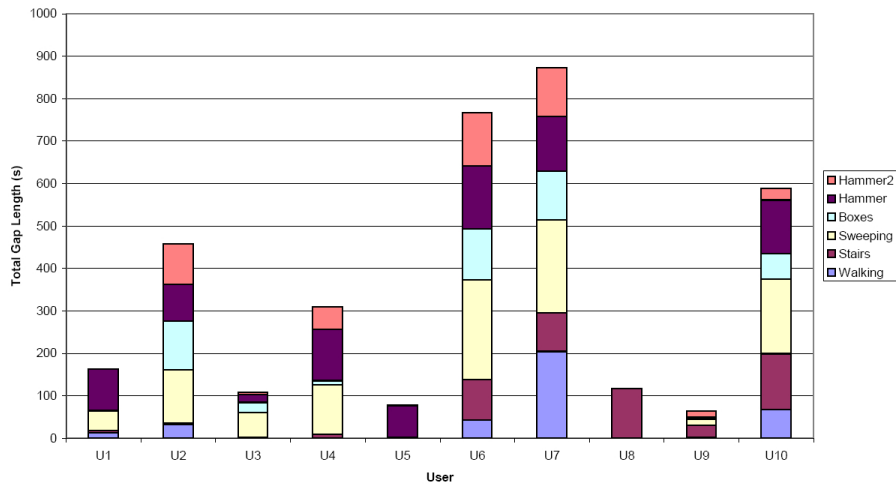


Figure 5.4: Individual Activity Contribution to Total Gap Time

Table 5.7: Grouping of Users by Total Gap Size

	Users	Total Gap Time	30% Loss Activities
I	U1,U3,U5,U8,U9	< 300s	< 1
II	U2,U4,U10	(300s - 600s)	≥ 3
III	U6,U7	> 600s	≥ 4

By virtue of the low total gap time, the helmet monitored better during each activity for users in Group I, whereas the monitoring in Group III was

poor on each activity, giving rise to those users' high total gaps. Exploring this further, we can ensure this trend is a property of the users themselves and not necessarily how long they performed the activity by normalizing each activity to its duration. In Figure 5.5 we see again that if a user performed well overall, then generally each activity lost a low percentage of the measurements. For the Users in Group I, they had at most one activity where 30% of data was lost, for Groups II and II there were 3 and 4 activities at 30% lost, respectively.

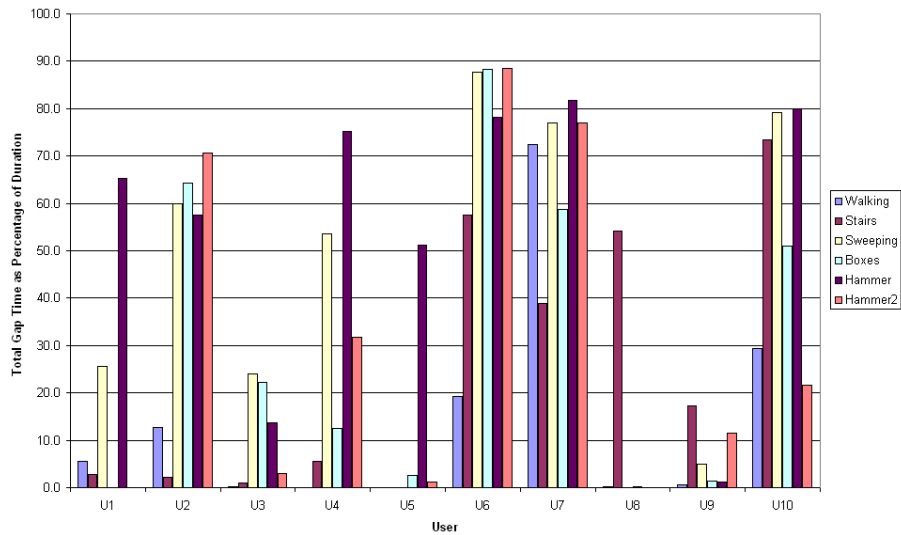


Figure 5.5: Total Gap Size as Percentage of Activity Duration

5.3 User Parameters

In this section we discuss three contributing items to understand the variations in user performance: the tightness of the helmet, the gait of the users, and the sensor measurement site.

The tightness of the helmet is a prime factor in how well the sensor performs. As Dresher found, there is an optimal sensor pressure at which a good pulse

can be detected [4]. If the pressure on the forehead is too great, then blood flow is cut off and no measurement is possible. However, if the sensor is not securely in contact with the forehead, then ambient light can corrupt the results. In the study, users were instructed to wear the helmet at their comfort level. Depending on their personal feel, they may have tightened the helmet too much or too little, moving away from an optimal pressure and potentially degrading the result. A curious note regarding the fit of the helmet, User 8 was one of the best monitored during the test. Before beginning the test he indicated that he previously held a job where wearing a safety helmet was common. It is possible his familiarity with the helmet allowed him a proper fit that was also functional for the sensor. While requiring further study, this is a hopeful indicator that those accustomed to wearing a helmet may produce better results than the results obtained from the study.

Considering the gait of the users, it is possible there is no correlation among activities as each user performed the activities differently. Returning to the performance of User 8, while having virtually no gaps in most activities, the user did have time lost while completing the Stairs task. Perhaps when ascending and descending stairs this person bobs his head, whereas in the other tasks he was more stable. While this cannot be verified, further studies involving motion capture could pinpoint potential differences among users.

Finally, conditions of the measurement site may cause poor readings if there is not sufficient perfusion in the tissues to allow a reading. In particular, User 7 indicated that he had a scar on his forehead near the site where the sensor would normally sit. The scar may have damaged the vascular bed and restricted blood flow to the site. If true, this could be the cause for User 7 having the largest gap size overall.

Chapter 6

Conclusion

A pulse oximeter has been integrated into a typical construction helmet to assess the feasibility of monitoring for exposure to carbon monoxide. Ten participants took part in a user study to characterize the performance of the helmet using simulated construction tasks. During the study, continuous measurements of the users were recorded to determine how the prototype performed under motion. As the user performed the activities, measurement gaps were created by periods of high motion when the oximeter could not determine a valid reading.

The distribution of these gaps was compared to worst-case estimate of time to impairment for construction workers to determine if the measurement gaps were so frequent that a worker becoming impaired would go unnoticed. This was shown not to be case as a worst case as the helmet would provide a reading in 99.66% of cases. For further assurance, the time to impairment could be halved, with the helmet still providing a reading in 99.03% cases.

While these results do not ensure absolute monitoring of workers, the time to impairment is very conservative and was derived for a very susceptible worker under very difficult conditions. Therefore, the high probability of measurement

at more than 99% indicates that helmet-based monitoring is a feasible safety platform worthy of further study.

6.1 Future Work

The most compelling area for further work is in advancing the design of the helmet insert and reducing the impact of motion. At present, the insert is made of simple materials and Velcro is used for attachment, however a more elegant solution should be found. Additionally, a new helmet design should be attempted that mechanically isolates the inner headband from the exterior protective shell. Because a headband design itself would suffer little motion artifacts, isolating the weight of the exterior helmet from sensor themselves should provide great advancements in resistance to motion.

Also, the helmet is not an individual solution, but part of a network of sensors on the construction site. As a person impaired by carbon monoxide may be unable to self-rescue, the sole use of a personal alert would not adequate. Future designs can incorporate a multi-modal alert that warns co-workers of a person in danger. This alert could include transmitting radio messages and warnings to summon distant help, or provide visual and audible clues to the location of the worker. These additions would not be a large extension as wireless capability is already integrated into the prototype and could be easily turned on in case of emergencies.

Finally, the results of this study need to be validated with a true CO-pulse oximeter. While the blood oxygen oximeter used is technologically equivalent, there is no substitution for direct validation of the helmet. Hopefully as time passes the SpCO monitors will be made available at lower prices and smaller form factors.

Bibliography

- [1] D. J. Lofgren, “Occupational carbon monoxide poisoning in the state of washington, 1994-1999,” *Applied Occupational and Environmental Hygiene*, vol. 17, no. 4, pp. 286–295, 2002.
- [2] S. Dorevitch, L. Forst, L. Conroy, and P. Levy, “Toxic inhalation fatalities in us construction workers, 1990 to 1999,” *Journal of Occupational and Environmental Medicine*, vol. 44, no. 7, pp. 657–662, July 2002.
- [3] M. J. Ellenhorn, *Ellenhorn’s Medical Toxicology*. Williams and Wilkins, 1997, ch. 66, pp. 1465–1476.
- [4] R. Dresher, “Wearable forehead pulse oximetry: Minimization of motion and pressure artifacts,” Master’s thesis, Worcester Polytechnic Institute, May 2006.
- [5] A. Nagre and Y. Mendelson, “Effects of motion artifacts on pulse oximeter readings from different facial regions,” *Proceedings of the IEEE 31st Annual Northeast Bioengineering Conference*, pp. 220 – 222, April 2005.
- [6] J. G. Webster, Ed., *Design of Pulse Oximeters*. Taylor Francis, Inc., 1997.
- [7] NIOSH, “Preventing carbon monoxide poisoning from small gasoline-powered engines and tools,” September 1996. [Online]. Available: <http://www.cdc.gov/NIOSH/carbon2.html>

- [8] M. Nitzan and H. Taitelbaum, "The measurement of oxygen saturation in arterial and venous blood," *IEEE Instrumentation and Measurement Magazine*, vol. 11, no. 3, pp. 9–15, June 2008.
- [9] S. J. Barker and K. Tremper, "The effect of carbon monoxide inhalation on pulse oximetry and transcutaneous p_{O_2} ," *Anesthesiology*, vol. 66, pp. 677–679, 1987.
- [10] Masimo Corporation, "Masimo spco products," 2010. [Online]. Available: <http://www.masimo.co.uk/spco/index.htm>
- [11] R. P. Buinevicius, "A three wavelength pulse oximeter for carboxyhemoglobin determination," Master's thesis, University of Wisconsin - Madison, 1987.
- [12] S. J. Barker, J. Curry, D. Redform, and S. Morgan, "Measurement of carboxyhemoglobin and methemoglobin by pulse oximetry," *Anesthesiology*, vol. 105, no. 5, pp. 892–897, November 2006.
- [13] L. Wang, B. P. Lo, and G.-Z. Yang, "Multichannel reflective ppg earpiece sensor with passive motion cancellation," *IEEE Transactions on Biomedical Circuits and Systems*, vol. 1, no. 4, December 2007.
- [14] Nonin Medical Inc., "Nonin fingertip oximeters," 2010. [Online]. Available: <http://www.nonin.com/product-listing/fingertip/>
- [15] Y. Mendelson and B. D. Ochs, "Noninvasive pulse oximetry utilizing skin reflectance photoplethysmography," *IEEE Transactions on Biomedical Engineering*, vol. 35, no. 10, pp. 798 – 805, October 1988.
- [16] S. Rhee, B.-H. Yang, and H. Asada, "Artifact-resistant power-efficient design of finger-ring plethysmographic sensors," *IEEE Transactions on Biomedical Engineering*, vol. 48, no. 7, pp. 795 –805, July 2001.

- [17] H. H. Asada, P. Shaltis, A. Reisner, S. Rhee, and R. C. Hutchinson, “Mobile monitoring with wearable photoplethysmographic biosensors,” *IEEE Engineering in Medicine and Biology Magazine*, vol. 22, no. 3, pp. 28–40, 2003.
- [18] S. Kunchon, T. Desudchit, and C. Chinrungrueng, “Comparative and evaluative the adaptive filter in motion artifact cancellation of pulse oximetry,” *Proceedings of the IEEE 35th Annual Northeast Bioengineering Conference*, pp. 1–2, April 2009.
- [19] Yong-Sheng Yan and Yuan-Ting Zhang, “An efficient motion-resistant method for wearable pulse oximeter,” *IEEE Transactions on Information Technology in Biomedicine*, vol. 12, no. 3, pp. 399–405, May 2008.
- [20] K. Reddy, B. George, and V. Kumar, “Use of fourier series analysis for motion artifact reduction and data compression of photoplethysmographic signals,” *IEEE Transactions on Instrumentation and Measurement*, vol. 58, no. 5, pp. 1706–1711, May 2009.
- [21] L. Wood and H. Asada, “Noise cancellation model validation for reduced motion artifact wearable ppg sensors using mems accelerometers,” *Proceedings of the 28th Annual International Conference of the IEEE Engineering in Medicine and Biology Society*, pp. 3525–3528, September 2006.
- [22] A. Relente and L. Sison, “Characterization and adaptive filtering of motion artifacts in pulse oximetry using accelerometers,” *Proceedings of the Second Joint EMBS/BMES Conference*, vol. 2, pp. 1769–1770, 2002.
- [23] G. Comtois, Y. Mendelson, and P. Ramuka, “A comparative evaluation of adaptive noise cancellation algorithms for minimizing motion artifacts in a forehead-mounted wearable pulse oximeter,” *Proceedings of the 29th*

Annual International Conference of the IEEE Engineering in Medicine and Biology Society, pp. 1528 –1531, August 2007.

- [24] R. Drescher and Y. Mendelson, “Reflectance forehead pulse oximetry: Effects of contact pressure during walking,” *Proceedings of the 28th Annual International Conference of the IEEE Engineering in Medicine and Biology Society*, pp. 3529 –3532, September 2006.
- [25] S. J. Barker, “Motion resistant pulse oximetry: A comparison of new and old models,” *Anesthesia & Analgesia*, vol. 95, pp. 967–972, 2002.
- [26] W. Johnston, P. Branche, C. Pujary, and Y. Mendelson, “Effects of motion artifacts on helmet-mounted pulse oximeter sensors,” *Proceedings of the IEEE 30th Annual Northeast Bioengineering Conference*, pp. 214 – 215, April 2004.
- [27] H. F. Martz and R. A. Waller, *Bayesian Reliability Analysis*. John Wiley & Sons, 1982.
- [28] M. Ananda and J. Gamage, “On steady state availability of a system with lognormal repair time,” *Applied Mathematics and Computation*, vol. 150, pp. 409–416, 2004.
- [29] M. Ananda, “Confidence intervals for steady state availability of a system with exponential operating time and lognormal repair time,” *Applied Mathematics and Computation*, vol. 137, pp. 499–509, 2003.
- [30] B. Schroeder and G. A. Gibson, “A large-scale study of failures in high-performance computing systems,” in *International Conference on Dependable Systems and Networks*, June 2006, pp. 249–258.

- [31] R. E. Mullen, “The lognormal distribution of software failure rates: Origin and evidence,” in *Proceedings of the 9th International Symposium on Software Reliability Engineering*, November 1998, pp. 124–133.
- [32] J. R. Llyod, “On the log-normal distribution of electromigration lifetimes,” *Journal of Applied Physics*, vol. 50, no. 7, pp. 5062–5064, July 1979.
- [33] K. Croes, J. V. Manca, W. D. Ceuninck, L. D. Schepper, and G. Molenbergs, “The time of guessing your failure distribution is over!” *Microelectronics Reliability*, vol. 38, no. 6-8, pp. 1187–1191, 1998.
- [34] R. F. Coburn, R. Forester, and P. Kane, “Considerations of the physiological variables that determine the blood carboxyhemoglobin concentration in man,” *Journal of Clinical Investigation*, vol. 44, no. 11, pp. 1899–1910, 1965.
- [35] T. Bernard and J. Duker, “Modeling carbon monoxide uptake during work,” *American Industrial Hygiene Association Journal*, vol. 42, no. 5, pp. 361–364, May 1981.
- [36] J. E. Peterson and R. D. Stewart, “Predicting the carboxyhemoglobin levels resulting from carbon monoxide exposures,” *Journal of Applied Physiology*, vol. 39, no. 4, pp. 633–638, October 1975.
- [37] P. Tikuisis, H. Madill, B. Gill, W. Lewis, K. Cox, and D. Kane, “A Critical Analysis of the Use of the CFK Equation in Predicting COHb Formation,” *American Industrial Hygiene Association Journal*, vol. 48, no. 3, pp. 208–213, March 1987.
- [38] W. D. McArdle and V. L. Katch, *Exercise Physiology: energy, nutrition and human performance*, 6th ed. Lippincott Williams and Wilkins, 2007.

- [39] World Health Organization, “Worldwide prevalence of anemia 1993-2005,” 2008. [Online]. Available: http://whqlibdoc.who.int/publications/2008/9789241596657_eng.pdf
- [40] —, “Iron deficiency anemia assessment, prevention, and control. a guide for program managers.” 2001. [Online]. Available: http://whqlibdoc.who.int/hq/2001/WHO_NHD_01.3.pdf
- [41] Y. Alari, “Toxicity of fire smoke,” *Critical Reviews in Toxicology*, vol. 32, no. 4, pp. 259–289, 2002.
- [42] P. Tikuisis, F. Buick, and D. M. Kane, “Percent carboxyhemoglobin in resting humans exposed repeatedly to 1,500 and 7,500 ppm CO,” *Journal of Applied Physiology*, vol. 63, no. 2, pp. 820–827, 1987.
- [43] P. Tikuisis, D. M. Kane, T. M. McLellan, F. Buick, and S. M. Fairburn, “Rate of formation of carboxyhemoglobin in exercising humans exposed to carbon monoxide,” *Journal of Applied Physiology*, vol. 72, no. 4, pp. 1311–1319, 1992.
- [44] Y. Mendelson, J. C. Kent, B. L. Yocum, and M. J. Birle, “Design and evaluation of a new reflectance pulse oximeter sensor,” *Medical Instrumentation*, vol. 22, no. 4, 1988.
- [45] Y. Mendelson and C. Pujary, “Measurement site and photodetector size considerations in optimizing power consumption of a wearable reflectance pulse oximeter,” *Proceedings of the 25th Annual International Conference of the IEEE Engineering in Medicine and Biology Society*, vol. 4, pp. 3016 – 3019, September 2003.
- [46] M. Nogawa, T. Kaiwa, and S. Takatani, “A novel hybrid reflectance pulse oximeter sensor with improved linearity and general applicability to various

- portions of the body,” *Proceedings of the 20th Annual International Conference of the IEEE Engineering in Medicine and Biology Society*, vol. 4, pp. 1858 –1861, 1998.
- [47] S. Rhee, B.-H. Yang, K. Chang, and H. Asada, “The ring sensor: a new ambulatory wearable sensor for twenty-four hour patient monitoring,” *Proceedings of the 20th Annual International Conference of the IEEE Engineering in Medicine and Biology Society*, vol. 4, pp. 1906 –1909, 1998.
- [48] E. Geun, H. Heo, K. C. Nam, and Y. Huh, “Measurement site and applied pressure consideration in wrist photoplethysmography,” *23rd Technical Conference on Circuits/Systems, Computers and Communications*, 2008.
- [49] Nonin Medical Inc., “Nonin xpod,” 2010. [Online]. Available: <http://www.nonin.com/OEMsolutions/Xpod>
- [50] W. Johnston and Y. Mendelson, “Investigation of signal processing algorithms for an embedded microcontroller-based wearable pulse oximeter,” *Proceedings of the 28th Annual International Conference of the IEEE Engineering in Medicine and Biology Society*, pp. 5888 – 5891, September 2006.
- [51] Digi International Inc, “Xbee products,” 2010. [Online]. Available: <http://www.digi.com/products/wireless/zigbee-mesh/>
- [52] SparkFun Electronics, “Xbee explorer regulated,” 2010. [Online]. Available: http://www.sparkfun.com/commerce/product_info.php?products_id=9132
- [53] Energizer Holdings, Inc., “Energizer 9v alkaline product datasheet,” 2009. [Online]. Available: <http://data.energizer.com/PDFs/522.pdf>

- [54] —, “Energizer 9v lithium product datasheet,” 2009. [Online]. Available: <http://data.energizer.com/PDFs/la522.pdf>
- [55] Microchip Technology, “Pic18f45j10 family datasheet,” 2009. [Online]. Available: <http://ww1.microchip.com/downloads/en/DeviceDoc/39682E.pdf>
- [56] H. L. Gray and W. R. Schucany, “Lower confidence limits for availability assuming lognormally distributed repair times,” *IEEE Transactions on Reliability*, vol. 18, no. 4, pp. 157–162, November 1969.